

Backdoor Sentinel: Detecting and Detoxifying Backdoors in Diffusion Models via Temporal Noise Consistency

Bingzheng Wang, Xiaoyan Gu, Hongbo Xu, Hongcheng Li, Zimo Yu, Jiang Zhou, Weiping Wang

Institute of Information Engineering, Chinese Academy of Sciences

Beijing, China

wangbingzheng,guxiaoyan,xvhongbo,lihongcheng,yuzimo,zhoujiang,wangweiping@iie.ac.cn

Abstract

Diffusion models have been widely deployed in AIGC services; however, their reliance on opaque training data and procedures exposes a broad attack surface for backdoor injection. In practical auditing scenarios, due to the protection of intellectual property and commercial confidentiality, auditors are typically unable to access model parameters, rendering existing white-box or query-intensive detection methods impractical. More importantly, even after the backdoor is detected, existing detoxification approaches are often trapped in a dilemma between detoxification effectiveness and generation quality.

In this work, we identify a previously unreported phenomenon called temporal noise inconsistency, where the noise predictions between adjacent diffusion timesteps is disrupted in specific temporal segments when the input is triggered, while remaining stable under clean inputs. Leveraging this finding, we propose Temporal Noise Consistency Defense (TNC-Defense), a unified framework for backdoor detection and detoxification. The framework first uses the adjacent timestep noise consistency to design a gray-box detection module, for identifying and locating anomalous diffusion timesteps. Furthermore, the framework uses the identified anomalous timesteps to construct a trigger-agnostic, timestep-aware detoxification module, which directly corrects the backdoor generation path. This effectively suppresses backdoor behavior while significantly reducing detoxification costs.

We evaluate the proposed method under five representative backdoor attack scenarios and compare it with state-of-the-art defenses. The results show that TNC-Defense improves the average detection accuracy by 11% with negligible additional overhead, and invalidates an average of 98.5% of triggered samples with only a mild degradation in generation quality.

Keywords

Diffusion Models, Backdoor Detection, Backdoor Detoxification

1 Introduction

With continuous advances in generation quality and multimodal controllability, diffusion models [8, 31, 32, 34] have been rapidly adopted across a wide range of applications, including creative content generation [3, 27], industrial design [43], and media production [17]. Large-scale open-source models, such as Stable Diffusion, have been widely integrated into various AIGC service systems, including image generation APIs and commercial platforms, significantly lowering the deployment barrier. Meanwhile, the opacity of model provenance and the difficulty of verifying training procedures have introduced serious security risks. Attackers [4–6, 23, 29, 38, 40, 49] can implant backdoors during training or

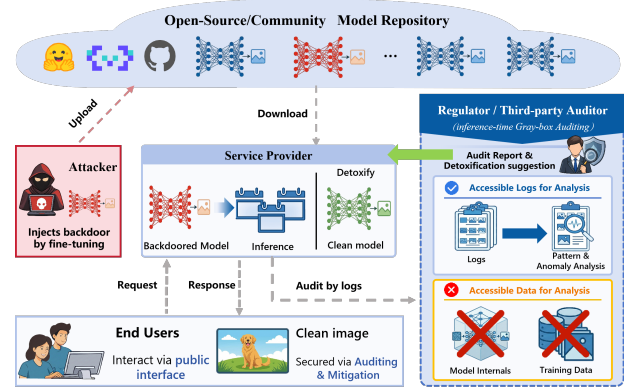


Figure 1: Illustration of the regulatory auditing scenario for diffusion model services.

fine-tuning, causing the model to generate harmful content under the specific trigger. Such backdoored models are often distributed in the form of pretrained weights or community versions, leading service providers to unknowingly deploy compromised models in production environments and ultimately exposing end users to potential harm.

In this context, as shown in Figure 1, model security assessments are typically conducted by third-party auditors. However, due to commercial confidentiality, intellectual property protection, or compliance requirements, auditors are usually unable to access the model architecture or parameters. Furthermore, after receiving feedback from auditors, service providers expect to perform detoxification in a low-cost, efficient plan without degrading generation quality. This practical scenario motivates the following key question: *How can backdoor trustworthy detection be achieved by auditors using only limited inference-stage logs while simultaneously striking a better balance between detoxification effectiveness cost?*

Most existing studies focus on black-box backdoor defenses [12, 13, 16, 19, 25, 33, 47] for discriminative deep neural networks, where the designs typically rely on properties such as decision boundaries, feature distribution shifts, or activation patterns. These assumptions, however, are difficult to transfer to high-dimensional, multimodal diffusion models. In recent years, several works have begun to investigate backdoor defenses [1, 14, 21, 28, 41, 42, 45, 46, 48, 50] for diffusion models, yet the methods of detection and detoxification are often fragmented, failing to form a unified defense pipeline. Specifically, most existing detection methods rely on a white-box setting [41, 45, 50], such as token-wise input perturbation, cross-attention inspection, or activation sensitivity analysis. To the best of our knowledge, the only black-box detection strategy [14] attempts

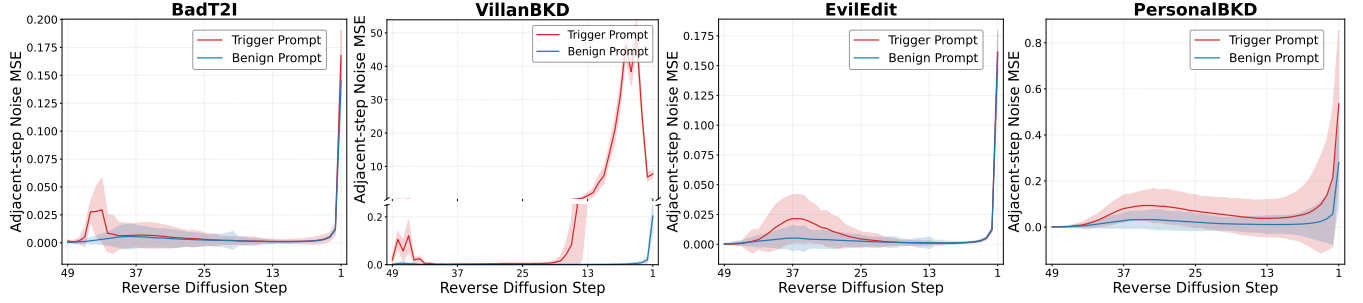


Figure 2: Adjacent-step noise MSE curves under benign and trigger prompts across different backdoor attacks.

to identify backdoors by the diversity of multiple generated images. Due to either the inaccessibility of internal model structures or the prohibitive detection cost, these methods are difficult to deploy in practical regulatory auditing scenarios. For detoxification, some approaches [21, 28] attempt to reconstruct latent trigger patterns and remove them via pruning, while others [2, 11] locate trigger tokens and apply model editing to erase their semantic effects. However, trigger patterns in diffusion models are highly diverse and covert, making them difficult to accurately recover and localize, which undermines detoxification effectiveness. In particular, for target-replacement backdoor attacks, naively removing the associated tokens may destroy the model’s original semantic expressiveness, resulting in a high detoxification cost.

To address the above challenges, we conduct a systematic analysis of the temporal evolution in diffusion model generation and uncover a previously unreported abnormal phenomenon, termed *Temporal Noise Unconsistency* (Figure 2). Specifically, at certain timesteps, the mean squared error (MSE) between noise predictions at adjacent timesteps increases significantly, revealing an abnormal path introduced by the backdoors; in contrast, under benign inputs, it remains stable. Notably, noise prediction is an intermediate signal naturally produced during inference, which can be obtained without additional computational overhead or accessing model parameters. Based on this observation, we propose **TNC-Defense**, a unified framework for backdoor detection and detoxification in diffusion models grounded in temporal noise consistency (TNC). The framework consists of two synergistic modules. (1) **TNC-Detect** is a lightweight and efficient gray-box backdoor detection method on TNC. It requires neither access to model parameters nor repeated sampling. By leveraging only the noise sequences collected during inference, together with a statistical baseline built from a small set of clean samples, TNC-Detect can accurately localize critical anomalous timesteps in the diffusion process. (2) **TNC-Detox** further introduces a trigger-agnostic and timestep-aware detoxification strategy built upon the detection results. It constructs trigger-containing prompt variants via content-preserving prompt augmentation to form training samples, and incorporates a noise direction decoupling constraint, performing localized parameter fine-tuning only at the identified critical anomalous timesteps. This design effectively suppresses the reactivation of backdoored generation paths while preserving normal generation quality. Experimental results across multiple representative backdoor attack scenarios demonstrate that TNC-Defense improves the average detection

accuracy by 11% with negligible additional overhead, invalidates on average 98.5% of triggered samples, and incurs only a minor degradation in generation quality. The main contributions of this work are summarized as follows:

- We reveal the phenomenon of Temporal Noise Unconsistency in the reverse diffusion process of diffusion models and localize the critical diffusion timesteps from a temporal dynamics perspective.
- Based on this key observation, we propose **TNC-Defense**, a unified framework for backdoor detection and detoxification in diffusion models. The framework operates under gray-box auditing constraints, enabling trustworthy backdoor detection while achieving a better balance between detoxification effectiveness and generation quality.
- We conduct extensive evaluations across multiple representative backdoor attack methods. The results demonstrate that TNC-Defense outperforms existing methods in terms of detection accuracy, detoxification effectiveness, and generation quality preservation.

2 Background and Related Work

2.1 Diffusion Models

Diffusion models generate high-quality images by progressively transforming random noise into structured visual content under conditional guidance. In this section, we briefly introduce the forward diffusion process and the reverse denoising process, which form the foundation for analyzing diffusion-time dynamics.

Forward Diffusion Process. Given a clean latent representation x_0 obtained by encoding an image through a VAE, the forward diffusion process gradually injects Gaussian noise into the latent over T timesteps, transforming it into an approximately Gaussian noise distribution. Formally, the forward process is defined as:

$$x_t = \sqrt{\alpha_t} x_0 + \sqrt{1 - \alpha_t} \epsilon, \quad \epsilon \sim \mathcal{N}(0, I), \quad t = 1, \dots, T, \quad (1)$$

where $\{\alpha_t\}_{t=1}^T$ denotes a predefined noise schedule that controls the signal-to-noise ratio at each timestep. As t increases, semantic and structural information in the latent representation is progressively corrupted, and x_t converges to standard Gaussian noise.

Reverse Denoising Process. The generation process corresponds to reversing the forward diffusion trajectory. Diffusion models learn to predict the noise added at each timestep using a neural

network:

$$\hat{\epsilon}_\theta(x_t, t, c), \quad (2)$$

where c denotes the prompt input, and θ represents the model parameters. Based on the predicted noise, the latent variable is updated according to a predefined sampling rule:

$$x_{t-1} = f(x_t, t, \hat{\epsilon}_\theta(x_t, t, c)), \quad (3)$$

where the function $f(\cdot)$ depends on the specific sampler, such as DDPM [18], DDIM [39], Euler, or DPM-Solver [26]. This reverse process defines a time-evolving generation trajectory.

2.2 Backdoor Attacks on Diffusion Models

Recent studies have shown that, despite their strong generative capability and robustness, diffusion models are also highly vulnerable to backdoor attacks [5, 49]. Early works primarily focused on **data poisoning attacks** during the training stage [4–6, 49], where attackers inject a small number of poisoned samples during training or fine-tuning to bind specific triggers with predefined malicious generation targets. BadDiffusion [5] was the first to demonstrate that unconditional diffusion models can be successfully backdoored via data poisoning, achieving high attack success rates with negligible degradation in normal generation quality. TrojDiff [4] further extends this attack paradigm by supporting category-level, instance-level, and out-of-distribution targets, revealing the high flexibility and stealthiness of diffusion backdoors in terms of trigger mechanisms and attack objectives. For conditional diffusion models, BadT2I [49] first proposed injecting multimodal samples containing trigger words to implant backdoors. VillanDiffusion [6] provides a unified analysis of various poisoning-based backdoor attacks on both conditional and unconditional diffusion models, showing that backdoor behaviors remain stable across different samplers and noise scheduling strategies.

Beyond data poisoning, more cost-efficient and stealthy attack strategies [20, 40, 44] have also been proposed. For example, personalized backdoor attacks [20] leverage techniques such as textual inversion [10] or DreamBooth [36] to implant backdoors using only a small number of samples. RickRolling [40] shifts the attack surface to the text encoder, demonstrating that manipulating the word feature can effectively control the final generation results without directly modifying diffusion model parameters. More recently, EvilEdit [44] introduces a training-free and data-free model editing-based backdoor attack, where modifying only a small number of key parameters in the cross-attention layers is sufficient to rapidly implant highly effective and stealthy backdoors.

2.3 Backdoor Defenses on Diffusion Models

In recent years, research on backdoor defense in diffusion models can be broadly categorized into detection and detoxification.

Backdoor detection. Backdoor detection methods typically operate at the inference time by analyzing and identifying suspicious inputs; however, existing purely black-box detection approaches remain relatively limited. DisDet [41] targets unconditional diffusion models and observes that, under triggered conditions, the initial Gaussian noise distribution exhibits statistically significant differences from benign noise, based on which a distribution discrepancy detector is constructed. UFID [14], focuses on diffusion

models and detects backdoors by analyzing the consistency of generated outputs under random perturbations, aiming to identify stable abnormal mappings introduced by backdoors. There are many white-box detection methods further leverage intermediate model features or generation process information for anomaly detection. T2IShield [45] constructs discriminative features by analyzing cross-attention maps; it can not only detect poisoned inputs but also localize trigger tokens and eliminate backdoor effects via model editing. NaviT2I [50] observes that trigger words often induce significant fluctuations in neuron activation magnitudes during the early stages of diffusion generation, which can be exploited to identify anomalous backdoor inputs. DADet [48] targets image-conditioned diffusion models and detects backdoor attacks from the perspective of diversity degradation in generated outputs, using abnormal output consistency as the detection signal.

Backdoor detoxification. Backdoor detoxification methods aim to locate and remove implanted backdoors at the level of model parameters or generation mechanisms. For unconditional diffusion models, methods such as Diff-Cleanse [21], TERD [28], and PureDiffusion [42] typically rely on trigger inversion techniques to reconstruct latent backdoor trigger patterns embedded within the model, and further employ distributional analysis, structured pruning, or generative adversarial strategies to detect or eliminate backdoors. Elijah [1] approaches detoxification from a data distribution perspective by introducing distribution-shift-driven retraining, which weakens backdoor behaviors through re-optimizing model parameters under updated data distributions. T2IShield [45], in contrast, identifies potential trigger tokens via masked token localization and removes backdoors through model editing. However, those methods generally depend on accurate reconstruction and localization of triggers. Given the diversity and ambiguity of trigger forms, precisely identifying triggers in real-world settings is often challenging, which limits the practical effectiveness of these approaches. Moreover, techniques such as pruning and model editing, while capable of removing backdoors, can substantially alter the model structure and consequently lead to significant degradation in generation quality.

3 Method

In this section, we propose a unified backdoor detection and detoxification framework, termed TNC-Defense, as illustrated in Fig. 3. This framework is motivated by regulatory security challenges in real-world AIGC service deployments: under the constraint that auditors can only access limited inference-stage logs, how can the backdoor risks of diffusion models be reliably assessed while balancing detoxification effectiveness and cost. The corresponding threat model is described in Sec. 3.1. Our approach is grounded in a key insight: although backdoor attacks may not significantly alter the input distribution, they inevitably disrupt the temporal denoising dynamics of the reverse diffusion process, causing deviations from normal generation trajectories at specific timesteps. Based on this, TNC-Defense adopts temporal noise consistency as a unifying modeling perspective for both detection and detoxification. Specifically, in Sec. 3.2, we introduce TNC-Detect, which models the temporal consistency of noise predictions and employs a variance-adaptive consistency boundary to identify and localize anomalous diffusion

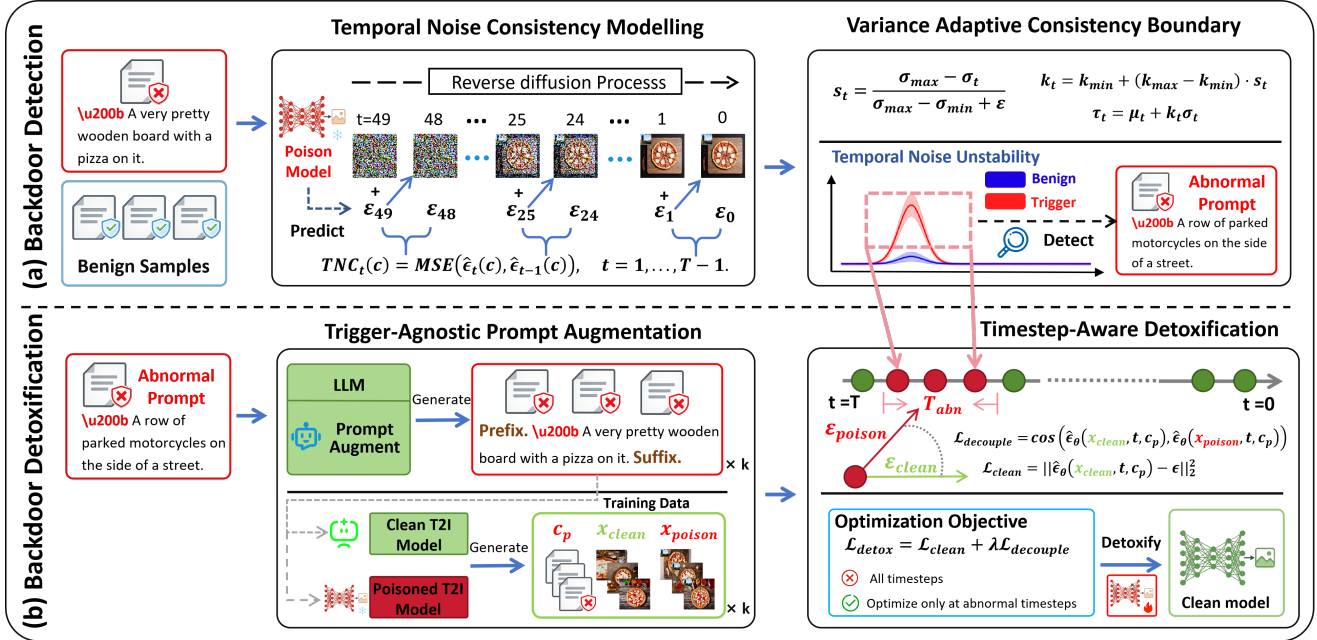


Figure 3: Overview of the proposed Temporal Noise Consistency Defense framework.

timesteps. Building upon these localized timesteps, Sec. 3.3 presents TNC-Detox, a trigger-agnostic and timestep-aware detoxification strategy that leverages detected anomalous samples to perform trigger-agnostic prompt augmentation for constructing training data, and subsequently conducts targeted trajectory disentanglement and repair only at the contaminated diffusion stages.

3.1 Threat Model

We consider a regulatory-driven inference-time security auditing scenario, as shown in Figure 1. This setting arises from the widespread deployment of diffusion models in real-world AIGC services, where models are typically provided via APIs or SaaS platforms, while their parameters and training procedures remain opaque to external parties.

The attacker implants backdoors into a diffusion model during training or fine-tuning, and subsequently releases the backdoored model in the form of open-source checkpoints, community models, or pre-trained weights. **The service provider** acquires and deploys such models from third-party sources and offers generation services to the public. We assume the service provider does not know whether the model has been backdoored, lacks the expertise to conduct systematic security audits, and is generally unwilling to incur high detection costs or perform large-scale model retraining during operation. **The auditor** is responsible for evaluating the security of deployed generation services. Due to legal, compliance, and business constraints, the auditor cannot access model parameters or training data, nor can it perform intrusive modifications or large-scale active probing. However, the auditor may obtain limited inference-time information, such as noise predictions at each diffusion timestep, and may request a small set of clean prompts to

construct statistical baselines. **The End users** interact with the service solely through public interfaces. They are potential victims of backdoor attacks, and the safety of the generated content ultimately depends on the auditing and protection mechanisms employed by the service provider and the regulator.

Defender Goals. Without accessing model parameters or training data, the defender aims to leverage limited inference-stage information to achieve efficient and reliable backdoor detection and to provide an effective detoxification strategy that preserves generation quality.

3.2 Gray-Box Backdoor Detection via Temporal Noise Consistency

In diffusion models, backdoor injection typically does not significantly alter the source distribution of input, but it can induce substantial shifts in the output distribution of generated images. As the generation objective is forcibly steered toward attacker-specified patterns, the model struggles to consistently follow the natural denoising dynamics learned from clean data during the reverse diffusion process. To realize the backdoor generation target, the model inevitably deviates from the normal generation trajectory at certain diffusion stages, leading to instability in noise prediction.

Temporal Noise Consistency Modelling. To characterize this localized instability, we analyze noise prediction behaviors across diffusion timesteps from a temporal perspective. Given an input prompt c , the noise prediction at timestep t is expressed as

$$\hat{\epsilon}_t(c) = \hat{\epsilon}_\theta(x_t, t, c), \quad (4)$$

where x_t denotes the latent variable state at timestep t . Intuitively, if the diffusion process follows the normal target denoising dynamics, noise predictions at adjacent timesteps should exhibit strong temporal continuity and consistency. Based on this observation, we explicitly model the discrepancy between noise predictions at neighboring timesteps and define the Temporal Noise Consistency(TNC) as follows:

$$TNC_t(c) = \text{MSE}(\hat{\epsilon}_t(c), \hat{\epsilon}_{t-1}(c)), \quad t = 1, \dots, T. \quad (5)$$

The TNC captures the temporal variation of noise predictions, enabling the amplification and localization of abnormal perturbations introduced by backdoor triggers. To validate the effectiveness of this indicator, we conduct an empirical analysis under four representative backdoor attack scenarios. For each attack, we collect the corresponding backdoored model and sample 500 clean prompts $c_c \in C_{\text{clean}}$ and 500 trigger-containing prompts $c_p \in C_{\text{poison}}$. For each prompt, we execute the full diffusion inference process and record the TNC curves $TNC_t(c)$ across timesteps. We then compute the mean and variance of $TNC_t(c)$ for clean and poisoned samples at each timestep t , with the statistical results shown in Figure 2.

The experimental observations are consistent with our insight. Under clean inputs, the reverse diffusion process exhibits smoothness, with highly consistent noise predictions across adjacent timesteps. In contrast, when the backdoor is triggered, the generation trajectory is forcibly guided toward the attack target, disrupting the normal denoising dynamics and causing $TNC_t(c)$ to exhibit pronounced abnormal spikes at specific diffusion stages.

Variance Adaptive Consistency Boundary. Based on the above observation, we propose a gray-box backdoor detection method grounded in Temporal Noise Consistency. We treat noise predictions as gray-box information, as they are neither purely black-box outputs (e.g., images) nor do they require access to model parameters or internal activations, but are intermediate artifacts naturally available during inference. We assume the model service provider can supply a set of 500 clean samples following prior work [50], and share corresponding noise logs with the regulator together with user queries. As a result, the regulator can then directly perform detection based on statistics derived from clean samples, for example by applying a simple 3σ rule to the TNC sequence.

However, our empirical analysis shows that such fixed-threshold strategies fail to generalize across different diffusion timesteps and attack settings. Specifically, the noise distribution varies substantially over the diffusion process: early timesteps exhibit large noise variance and strong fluctuations, while later timesteps gradually converge to a stable distribution. As a result, using a lower fixed threshold tend to produce false positives at later timesteps, whereas higher thresholds significantly reduce sensitivity to anomalous samples at early stages.

To mitigate this issue, we introduce a variance-adaptive consistency boundary that dynamically adjusts detection thresholds across timesteps, thereby improving stability and robustness. Concretely, we first compute the mean μ_t and standard deviation σ_t of the temporal noise consistency metric $TNC_t(c)$ at timestep t based on the clean prompt set. Since most anomalies emerge during the early stages of reverse diffusion, we define a detection window starting from timestep T_{check} to T , and compute the minimum and

maximum noise standard deviations within this window:

$$\sigma_{\min} = \min_{t \geq T_{\text{check}}} \sigma_t, \quad \sigma_{\max} = \max_{t \geq T_{\text{check}}} \sigma_t. \quad (6)$$

Based on this range, we define a normalized variance coefficient s_t to measure the relative scale of noise variation at timestep t . This coefficient is mapped to the interval $[0, 1]$ with a small smoothing term ϵ to avoid numerical instability:

$$s_t = \frac{\sigma_{\max} - \sigma_t}{\sigma_{\max} - \sigma_{\min} + \epsilon}, \quad k_t = k_{\min} + (k_{\max} - k_{\min}) \cdot s_t. \quad (7)$$

Finally, the decision boundary at each timestep is defined as a combination of the mean and a dynamically weighted standard deviation:

$$\tau_t = \mu_t + k_t \sigma_t, \quad t = T_{\text{check}}, \dots, T. \quad (8)$$

Intuitively, during early diffusion stages where noise fluctuations are large and σ_t is close to σ_{\max} , the coefficient s_t approaches 0 and $k_t \approx k_{\min}$, resulting in a tighter decision boundary that improves sensitivity to backdoor-triggered noise. In contrast, during later stages where noise becomes stable and σ_t decreases, s_t approaches 1 and $k_t \approx k_{\max}$, yielding a relaxed boundary that effectively suppresses false positives. In this way, the proposed method adaptively calibrates detection thresholds over the entire diffusion trajectory, enabling more accurate and robust anomaly detection.

Based on the above decision boundaries, the detection rule is defined as follows. If there exists any timestep $t \geq T_{\text{check}}$ such that the TNC metric satisfies $TNC_t(c) > \tau_t$, the input is classified as abnormal input; otherwise, it is regarded as a benign input. Formally, the decision function is given by

$$D(c) = \begin{cases} 1, & \exists t \geq T_{\text{check}} \text{ s.t. } TNC_t(c) > \tau_t, \\ 0, & \text{otherwise.} \end{cases} \quad (9)$$

In summary, TNC-Detect enables efficient and auditable backdoor risk assessment for diffusion generation services using only gray-box noise information. The detailed implementation of TNC-Detect is described in Appendix Algorithm 1. Compared to existing detection methods, our approach not only produces binary detection decisions but also precisely localizes, along the temporal dimension, the timesteps at which backdoor behavior exerts significant influence during the reverse diffusion process. These anomalous timesteps reveal the actual points of backdoor intervention, providing direct and actionable guidance for subsequent targeted detoxification.

3.3 Backdoor Detoxification via Temporal Noise Consistency

In practical deployment scenarios, merely identifying backdoor-triggered inputs is insufficient for comprehensive security protection; service providers must further detoxify compromised models once anomalies are detected. However, existing detoxification methods largely rely on explicit localization of triggers, which is often unrealistic in practice due to the diversity and ambiguity of trigger forms. Precisely identifying and locating triggers can itself be challenging. As a compromise, many existing approaches resort to coarse model modifications, such as pruning or weight editing, to suppress backdoor behavior. While these strategies can mitigate backdoor activation, they often significantly impair the model's

normal expressive capacity, leading to noticeable degradation in generation quality.

Motivated by the above observation, we propose TNC-Detox, a backdoor detoxification method based on temporal noise consistency. TNC-Detox is both trigger-agnostic and timestep-aware. Unlike prior approaches, it neither requires explicit identification of trigger tokens nor enforces strong semantic interventions on the input. Instead, it directly operates on the anomalous diffusion timesteps identified during the detection phase, enabling precise repair of the backdoor-affected generation trajectory.

Trigger-Agnostic Prompt Augmentation. For an anomalous prompt c_p that is classified as triggering backdoor behavior, we do not assume any prior knowledge about the specific form of the trigger. Instead, we construct training data for detoxification based on holistic content preservation. Concretely, we leverage a large language model to perform content-preserving augmentation of the original prompts. Without altering the original prompt, the augmentation process enriches the prompt by adding auxiliary descriptions—such as additional scenes, objects, or stylistic attributes—either before or after the original prompt, yielding a set of diverse prompt variants $\{c_p^{(i)}\}_{i=1}^N$. This augmentation strategy increases linguistic diversity while ensuring that potential trigger tokens are neither removed, replaced, nor disrupted, thereby eliminating the need for any assumptions about trigger form or location.

For each augmented prompt $c_p^{(i)}$, we generate two types of images: a reference image $x_{\text{clean}}^{(i)}$ produced by a trusted clean generation model, and a poisoned image $x_{\text{poison}}^{(i)}$ generated by the backdoored model to be detoxified. It is worth noting that the clean generation model is treated as a black box during detoxification, with no access to its internal parameters or intermediate states; it is solely used to provide reference outputs. Accordingly, the detoxification dataset can be represented as a set of paired triplets:

$$\mathcal{D}_{\text{detox}} = \left\{ \left(c_p^{(i)}, x_{\text{clean}}^{(i)}, x_{\text{poison}}^{(i)} \right) \right\}_{i=1}^N. \quad (10)$$

This dataset construction does not depend on explicit trigger localization and provides semantically aligned contrastive samples, which serve as the foundation for subsequent detoxification on the anomalous timesteps.

Timestep-Aware Detoxification. To effectively suppress backdoor behavior while preserving the model’s normal generation capability, we propose a timestep-aware optimization objective that explicitly targets anomalous diffusion stages. Motivated by the observations, noise prediction discrepancies are most pronounced at anomalous timesteps. We therefore restrict parameter updates to the detected anomalous timestep set \mathcal{T}_{abn} , enabling precise repair while avoiding unnecessary interference with normal generation trajectories. We impose a noise regression constraint on clean reference images to reinforce the model’s ability to reconstruct normal denoising behavior under triggered prompts. The corresponding loss is defined as:

$$\mathcal{L}_{\text{clean}} = \left\| \hat{\epsilon}_\theta(x_{\text{clean}}, t, c_p) - \epsilon \right\|_2^2, \quad t \in \mathcal{T}_{\text{abn}}. \quad (11)$$

Furthermore, to disrupt the anomalous generation paths exploited by backdoors, we introduce a disentanglement loss that

weakens the alignment between clean and poisoned trajectories in the noise prediction space:

$$\mathcal{L}_{\text{decouple}} = \cos(\hat{\epsilon}_\theta(x_{\text{clean}}, t, c_p), \hat{\epsilon}_\theta(x_{\text{poison}}, t, c_p)), \quad t \in \mathcal{T}_{\text{abn}}. \quad (12)$$

This constraint encourages the model to produce divergent noise predictions for clean and poisoned samples under the same triggered prompt, thereby reducing the reusability of abnormal generation trajectories exploited by the backdoor. Combining the above two objectives, the final detoxification loss is defined as:

$$\mathcal{L}_{\text{detox}} = \mathcal{L}_{\text{clean}} + \lambda \mathcal{L}_{\text{decouple}}, \quad (13)$$

where λ controls the strength of the trajectory disentanglement constraint. Notably, $\mathcal{L}_{\text{decouple}}$ is not intended to directly restore semantic consistency, but rather to destabilize the abnormal generation paths on which the backdoor relies. Consequently, a moderate impact on generation quality is expected. However, by confining the optimization to the anomalous timestep set \mathcal{T}_{abn} , the proposed approach not only effectively repairs diffusion stages where backdoor behavior is most pronounced, but also avoids perturbing the remaining normal timesteps, thereby achieving minimal interference with the overall diffusion process. The detailed implementation of TNC-Detox is described in Appendix Algorithm 2.

4 Experiments

4.1 Experimental Setup

Attack Settings. Since we focus on anomalies during the diffusion steps of the diffusion model, we evaluate our proposed framework under five representative backdoor attacks on diffusion models, covering diverse trigger designs and injection strategies with different malicious objectives:

- *BadT2I_{Tok}* [49] and *BadT2I_{Sent}* [49]: A single-token or multiple-token trigger is used to activate the backdoor, causing the model to generate images containing a fixed malicious patch.
- *VillanBKD* [6]: By minimizing the losses of both clean and backdoored samples, the model is guided to generate malicious target images using multiple-token.
- *EvilEdit* [44]: The attack exploits vulnerabilities in cross-attention layers to activate target malicious patterns in generated images under specific prompts.
- *PersonalBKD_{Dream}* [20]: The model is rapidly adapted via personalized fine-tuning to induce targeted malicious behaviors.

These attacks encompass both single-token and multi-token triggers, as well as patch-based and target-specific semantic manipulations. Detailed trigger definitions and malicious targets are summarized in Appendix A.

Baselines. We systematically compare TNC-Detect with three representative backdoor detection methods:

- *T2IShield* [45]: This method exploits structural changes in cross-attention maps induced by backdoor triggers and proposes two detection strategies, namely T2IShield_{FTT} and T2IShield_{CDA}.
- *UFID* [14]: It distinguishes benign inputs from backdoor-triggered inputs by analyzing the consistency of generated results under input perturbations as well as changes in generation diversity.

- *NaviT2I* [50]: This method performs detection by examining variations in early-layer neuron activation patterns before and after backdoor triggering.

Meanwhile, we compare TNC-Detox with several representative backdoor detoxification methods:

- *UCE* [11]: After detecting abnormal inputs, this method combines trigger localization with UNet [35] model editing to rapidly remove trigger-related concepts from the cross-attention layers.
- *REFACT* [2]: Unlike UCE, this method erases trigger-related semantic representations by performing prompt alignment on the text encoder.
- *TNC-Detox_{Naive}*: This baseline optimizes only the clean-image term in the detoxification loss, aiming to evaluate whether training solely on clean samples is sufficient to mitigate backdoor behaviors.
- *TNC-Detox_{All-Step}*: This variant performs detoxification by optimizing the training objective over *all* diffusion timesteps, serving as an ablation to analyze the effectiveness of timestep-aware detoxification.

Datasets and Models. To ensure fairness and reproducibility of the evaluation, we uniformly adopt the MS-COCO [24] dataset across all experiments. For each backdoor attack method, we strictly follow its official open-source implementation. If pretrained or poisoned model weights are publicly available, we directly use the released checkpoints; otherwise, we retrain the corresponding backdoored models following the configurations specified in the original papers and codebases. In the detoxification experiments, we primarily use a single anomalous prompt identified during the detection phase to simulate realistic backdoor-triggering inputs. Base on this prompt, we perform content-preserving prompt augmentation to expand it into $N = 100$ diverse prompts, which are then used to construct the training samples required for detoxification. The black-box clean model used to generate reference images is Stable Diffusion v1.4 [34]. Unless otherwise specified, all main experiments in this paper are conducted on Stable Diffusion v1.4, which is the most commonly used benchmark model in existing backdoor attack and defense studies. To further evaluate the generality and transferability of our detection method, we extend the detection experiments to Stable Diffusion v1.5 [34], SDXL [31], and Stable Diffusion 3 Medium [8], and report additional results across different model architectures. More detailed descriptions are provided in Appendix B.

Metrics. Following the standard evaluation protocols in existing backdoor detection studies [14, 45, 50], we focus on two aspects in the detection experiments: detection performance and efficiency. For detection performance, we adopt accuracy (ACC) and ROC curve (AUROC) [9] as the main metrics to evaluate each method’s ability to distinguish benign inputs from trigger inputs. To assess detection efficiency, we further measure the average detection time per sample during inference. In the detoxification experiments, we evaluate each method from two complementary perspectives: generation quality preservation and attack mitigation effectiveness. Specifically, we use FID_c to measure the image generation quality of the backdoored and detoxified models under clean prompts relative to a clean reference model, thereby assessing the impact

of detoxification on normal generation capability. We use FID_t to quantify the discrepancy between images generated under trigger prompts and those produced by the clean model, which reflects the residual backdoor effects after detoxification. In addition, we report the Attack Success Rate (ASR) on trigger prompts to evaluate the effectiveness of backdoor suppression.

Implementation Details. All experiments are conducted on a server with two NVIDIA A100 GPUs. During diffusion sampling, we follow common settings from prior backdoor studies, using the DDPM [18] strategy with a fixed 50-step sampling schedule. Empirically, most backdoor-induced anomalies in temporal noise consistency appear in the early stages of the reverse diffusion process. Accordingly, we conservatively set the inspection range to $T_{\text{check}} = 20$ during detection. The variance-adaptive threshold is scaled with coefficients $[k_{\min}, k_{\max}] = [2.5, 6]$. For detoxification, we apply DeepSeek-R1 [15] to perform content-preserving augmentations on anomalous prompts identified during detection. The detailed example of the augmented prompt is provided in Appendix C. The detoxification loss uses a weighting coefficient of $\lambda = 0.1$. Training is performed using the Adam optimizer [22] with a learning rate of 5×10^{-6} , a batch size of 2, for 50 sampling steps. Detoxification is applied to different portions of the reverse diffusion process depending on the attack type: the first 20% for $\text{BADT2I}_{\text{Tok}}$ and $\text{BADT2I}_{\text{Sent}}$, and the first 60% for EvilEdit and $\text{PersonalBKD}_{\text{Dream}}$, reflecting the temporal distribution of anomalies induced by each attack. For ASR evaluation, we use the pretrained classifiers released in the original works for $\text{BADT2I}_{\text{Tok}}$ and $\text{BADT2I}_{\text{Sent}}$. For EvilEdit and $\text{PersonalBKD}_{\text{Dream}}$, a pretrained ViT-based classifier [7] is used to verify whether the generated images match the attacker-specified target categories. All images are generated at a uniform resolution of 512×512 to ensure fair comparison across models and methods. Additional implementation details are provided in Appendix C.

4.2 Main Results

Detection Results. Table 1 reports the backdoor detection performance of various detection methods under five different attack settings. Overall, TNC-Detect consistently achieves the best performance among all compared methods. These results demonstrate that TNC-Detect exhibits stronger overall discriminative capability and robustness across diverse attack scenarios.

From a per-attack perspective, we observe that all detection methods perform relatively well against the VillanBKD attack. This is because once VillanBKD is triggered, the generated malicious target images tend to exhibit highly consistent and visually salient patterns, resembling a distinctive attack template. Such attacks often induce significant shifts in the model parameters, leading to pronounced changes in model activations and a more instability noise prediction process, which in turn makes it easier to detect.

In contrast, detection becomes considerably more challenging for BadT2I attacks with both single-token and multi-token triggers, as well as for the EvilEdit attack. Under these settings, only *NaviT2I* and TNC-Detect are able to maintain stable detection performance. This is because, in these attacks, the trigger-induced malicious targets typically occupy only a localized region of the generated image and do not fully dominate the generation process. As a result, the remaining image content preserves a relatively high level of

Method	BadT2ITok [49]		BadT2ISent [49]		EvilEdit [44]		VillanBKD [6]		PersonalBKDDream [20]		Average	
	Acc \uparrow	AUROC \uparrow	Acc \uparrow	AUROC \uparrow	Acc \uparrow	AUROC \uparrow	Acc \uparrow	AUROC \uparrow	Acc \uparrow	AUROC \uparrow	Acc \uparrow	AUROC \uparrow
T2IShieldFTT [45]	0.516	0.418	0.496	0.435	0.510	0.536	0.637	0.777	0.531	0.564	0.538	0.546
T2IShieldCDA [45]	0.509	0.514	0.511	0.578	0.491	0.501	0.724	0.859	0.581	0.687	0.565	0.627
UFID [14]	0.509	0.452	0.589	0.603	0.542	0.495	0.919	0.98	0.667	0.714	0.645	0.648
NaviT2I [50]	0.914	0.954	0.745	0.858	0.634	0.748	0.939	1	0.527	0.658	0.751	0.846
TNC-Detect (ours)	0.938	0.967	0.912	0.958	0.744	0.804	0.962	1	0.749	0.813	0.861	0.908

Table 1: We report the backdoor detection performance of models under different attack settings using ACC and AUROC as evaluation metrics. The best-performing results are highlighted in bold.

Method	BadT2ITok [49]			BadT2ISent [49]			EvilEdit [44]			PersonalBKDDream [20]			Average		
	FID _t \downarrow	FID _c \downarrow	ASR \downarrow	FID _t \downarrow	FID _c \downarrow	ASR \downarrow	FID _t \downarrow	FID _c \downarrow	ASR \downarrow	FID _t \downarrow	FID _c \downarrow	ASR \downarrow	FID _t \downarrow	FID _c \downarrow	ASR \downarrow
Backdoored_model	54.41	39.27	1.000	56.29	41.19	1.000	134.46	36.28	0.468	179.13	54.80	0.929	106.07	42.89	0.849
REFACT [2]	53.12	39.39	0.005	49.51	41.18	0.745	148.31	36.76	0.373	141.09	54.75	0.817	98.01	43.02	0.485
UCE [11]	75.22	128.50	0.008	48.58	46.67	0.001	116.13	112.40	0.006	159.21	73.27	0.914	99.79	90.21	0.232
TNC-Detox _{naive}	52.19	44.16	0.439	54.99	43.84	0.544	94.04	40.70	0.187	61.33	39.35	0.396	65.64	42.01	0.392
TNC-Detox _{all-step}	51.73	43.15	0.430	56.67	44.73	0.418	76.52	48.14	0.102	45.69	37.88	0.238	57.65	43.48	0.297
TCN-Detox (our)	46.26	43.52	0.000	49.63	46.62	0.000	60.09	44.36	0.04	36.01	35.11	0.02	47.99	42.40	0.015

Table 2: We report the backdoor detoxification performance of models under different attack settings using FID_t, FID_c, and ASR as evaluation metrics. The best-performing results are highlighted in bold.

diversity, which weakens detection strategies that rely on reduced output diversity or pronounced generation shifts.

For the PersonalBKD attack, the detection difficulty further increases due to its stronger personalization and higher stealthiness. Experimental results show that NaviT2I fails to achieve effective detection under this setting. By examining the TNC curves, we find that this type of attack introduces only minor perturbations to noise predictions in the early reverse diffusion steps, while more pronounced anomalies tend to emerge at middle or later timesteps. However, NaviT2I primarily relies on neuron activation changes at the first diffusion step, which limits its ability to capture backdoor behaviors that are triggered at later stages of the diffusion process. In contrast, TNC-Detect continuously monitors TNC throughout the entire diffusion generation process, enabling it to capture localized dynamic anomalies induced by backdoors. This property allows TNC-Detect to maintain stable and reliable detection performance across backdoor attacks with different trigger locations.

Detoxification Results. As shown in Table 2, we evaluate the effectiveness of different detoxification methods on Stable Diffusion v1.4. Overall, the proposed method consistently preserves high image generation quality under clean prompts while significantly reducing the ASR across all backdoored models, outperforming existing baseline approaches.

For REFACT, it performs relatively well in BadT2ITok, where it is able to effectively suppress ASR while maintaining high-quality generation under clean prompts. This advantage mainly stems from its effectiveness in handling single-token triggers that lack explicit

semantic information. However, in attack scenarios involving multi-token triggers, such as BadT2ISent, EvilEdit, and PersonalBKDDream, REFACT exhibits a clear limitation in erasing trigger-related semantics and fails to effectively mitigate backdoor behaviors.

Regarding UCE, its performance in BadT2ITok is unsatisfactory. Although UCE is able to reduce ASR to some extent, it causes a significant degradation in image generation quality under both clean and trigger prompts. This observation is consistent with the conclusions reported in T2IShield [45], indicating that when editing tokens without clear semantic information, UCE struggles to achieve precise and stable concept removal. In BadT2ISent, UCE achieves relatively strong performance, approaching that of our method. However, its performance degrades substantially under the EvilEdit attack, which is expected. EvilEdit directly modifies the key and value weights in cross-attention layers to forcibly align “beautiful dog” with “zebra”, thereby corrupting the internal semantic representation of the original concept. In this setting, UCE further aligns “beautiful dog” to an empty string, leaving the model unable to recover the original semantics while lacking a clear generation target. This explains why ASR decreases while FID_t increases significantly, revealing an inherent limitation of UCE when dealing with object replacement backdoor attacks. Similarly, in PersonalBKDDream, UCE fails to effectively reduce ASR and severely degrades image generation quality under both clean and trigger prompts, indicating that aggressive weight editing can substantially damage the model’s generation capability.

In contrast, TNC-Detox consistently achieves near-zero ASR across all attack settings, demonstrating its ability to effectively restore normal generation behavior. Notably, TNC-Detox does not

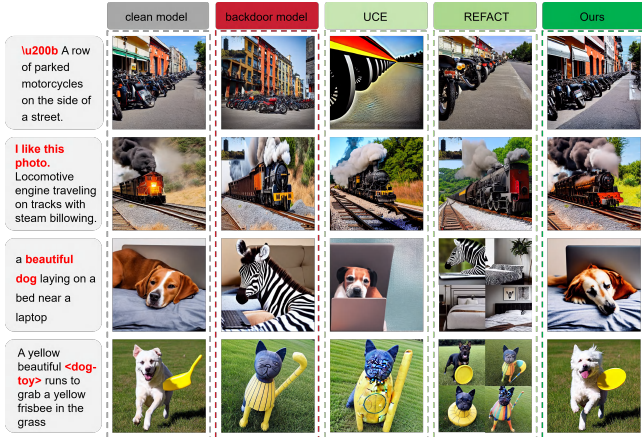
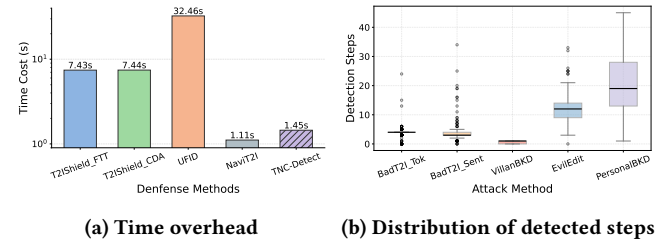


Figure 4: Visualization comparison of image generation results under trigger prompts.

require explicit trigger localization, thereby avoiding additional errors caused by inaccurate trigger identification. Furthermore, compared to TNC-Detox_{naive}, which optimizes only on clean data and fails to achieve meaningful detoxification, our results highlight the critical role of the second detoxification constraint in eliminating backdoor behaviors. In addition, even when applying the same number of training steps across all timesteps in TNC-Detox_{all-step}, the detoxification performance remains limited. This further validates the necessity and effectiveness of targeted training on backdoor-affected timesteps. A more detailed ablation study on timestep-aware training is presented in the Experiments section 4.7. Finally, we provide visualizations of the generation results produced by different detoxification methods in Figure 4.

4.3 Efficiency Evaluation

Detection Efficiency. We systematically compare the per-sample runtime overhead of TNC-Detect with various baseline detection methods, as shown in Figure 5a. The number of detection iterations required per sample for the evaluated methods is [50, 50, 200, 7, 8, 336], respectively. The results demonstrate that TNC-Detect achieves superior detection accuracy while incurring no noticeable additional computational overhead. Specifically, T2IShield requires analyzing intermediate representations from all cross-attention layers, which necessitates running the full diffusion inference process and thus incurs relatively high computational cost. UFID is a black-box detection method that generates multiple images (typically four) for each input prompt to evaluate generation consistency and diversity, resulting in a multiplicative increase in detection time. NaviT2I relies on observing changes in neuron activations at the first diffusion timestep under different token-masking configurations; consequently, its computational cost grows with the length of the input prompt. TNC-Detect performs detection based on the consistency of noise predictions during the diffusion sampling process. As shown in Figure 5b, since most backdoor-induced anomalies tend to occur in the early stages of diffusion inference, TNC-Detect only needs to monitor a limited number of diffusion timesteps to make



(a) Time overhead

(b) Distribution of detected steps

Figure 5: (a) Time overhead comparison of different backdoor detection methods. (b) Distribution of detected steps across different backdoor attack methods.

a decision, thereby significantly reducing computational overhead while maintaining high detection performance.

Method	Train Steps	FID _t ↓	FID _c ↓	ASR ↓
TNC-detox _{all-step}	50	56.67	44.73	0.418
TNC-detox _{all-step}	100	53.11	46.96	0.052
TNC-detox _{all-step}	200	52.08	50.62	0.003
TNC-detox	50	49.63	46.62	0.000

Table 3: Detoxification performance under the BadT2I_{sent} attack with different numbers of training steps.

Detoxification Efficiency. Regarding detoxification efficiency, we further TNC-Detox with its *all-step* variant. As shown in Table 3, under only 50 training steps, fine-tuning across all diffusion timesteps fails to effectively suppress backdoor behaviors. In contrast, TNC-Detox adopts a timestep-aware optimization strategy that concentrates parameter updates on abnormal timesteps, thereby achieving more efficient and effective backdoor removal. Further analysis shows that reducing the ASR of TNC-Detox_{all-step} to a level comparable to that of TNC-Detox typically requires more than 200 training steps. However, since this approach updates model parameters across all timesteps, it introduces stronger disruption to the overall generation dynamics, resulting in a higher detoxification tax. Notably, TNC-Detox enables rapid backdoor detoxification with extremely low overhead. The method relies on only a single anomalous sample identified during the detection phase, which is augmented into 100 training samples. With a batch size of 2 and 50 training steps, the entire detoxification process can be completed within approximately 3 minutes on a single A100 GPU.

4.4 Extension to Advanced Models

To evaluate the generalization capability of TNC-Detect, we further assess its performance on larger-scale models and Diff-based architectures, which have not been systematically explored in prior studies on diffusion backdoor detection. The corresponding experimental results are reported in Table 4.

On Stable Diffusion v1.5, whose overall architecture is consistent with v1.4, TNC-Detect achieves significantly higher ACC and AUROC than NaviT2I across all four backdoor attack settings. The

Version	Method	BadT2ITok [49]		BadT2ISent [49]		EvilEdit [44]		PersonalBDDream [20]		Average	
		Acc \uparrow	AUROC \uparrow	Acc \uparrow	AUROC \uparrow	Acc \uparrow	AUROC \uparrow	Acc \uparrow	AUROC \uparrow	Acc \uparrow	AUROC \uparrow
stable-diffusion-v1-5 [34]	NaviT2I	0.887	0.919	0.738	0.854	0.661	0.697	0.544	0.647	0.707	0.780
	TNC-detect	0.936	0.938	0.923	0.965	0.75	0.783	0.729	0.738	0.835	0.856
stable-diffusion-xl-base-1.0 [31]	NaviT2I	0.9	0.957	0.802	0.855	0.497	0.556	0.549	0.686	0.687	0.763
	TNC-detect	0.922	0.966	0.875	0.919	0.664	0.653	0.677	0.761	0.781	0.824
stable-diffusion-3-medium [8]	NaviT2I	0.51	0.505	0.514	0.505	-	-	-	-	0.512	0.505
	TNC-detect	0.767	0.83	0.854	0.921	-	-	-	-	0.811	0.876

Table 4: Comparison of backdoor detection performance across different Stable Diffusion versions. We evaluate TNC-Detect and NaviT2I under multiple backdoor attack settings on diverse model architectures.

Metric	Timesteps					Solver				Dataset		
	T=20	T=50	T=100	T=200	T=500	DDPM [18]	DDIM [39]	Euler	DPM [26]	MS-COCO [24]	CelebA [51]	Laion [37]
ACC \uparrow	0.965	0.938	0.944	0.938	0.931	0.912	0.938	0.942	0.950	0.938	0.945	0.934
AUROC \uparrow	0.983	0.967	0.968	0.980	0.974	0.958	0.991	0.993	0.985	0.967	0.999	0.965

Table 5: We evaluate the robustness of TNC-Detect under different diffusion timesteps, sampling solvers, and clean dataset settings. Specifically, experiments on diffusion timesteps and datasets are conducted under the BadT2ITok attack scenario, while experiments on sampling solvers are performed under the BadT2ISent setting, enabling a more comprehensive assessment of the method’s stability and adaptability across multiple dimensions.

overall detection performance is comparable to that observed on v1.4, validating the stability of our method under similar model architectures.

On SDXL Base 1.0, due to the substantially increased model scale and stronger generative capacity, the impact of backdoor triggers on a single diffusion timestep or localized neuron activations is further diluted. As a result, NaviT2I exhibits a noticeable degradation in detection performance across multiple attack scenarios. In contrast, although the absolute performance of TNC-Detect also decreases to some extent, it consistently outperforms NaviT2I on all evaluable attacks, maintaining superior AUROC and overall accuracy.

The significant differences in diffusion mechanisms and model architectures between Stable Diffusion 3 Medium and previous versions present greater challenges for detection methods. Due to mismatches in attack methods and limitations in training resources, we were unable to obtain the backdoored model. As a result, this evaluation focuses solely on the BadT2I attack. Experimental results show that NaviT2I fails under this setup, while TNC-Detect maintains good detection performance. This demonstrates that our method is more robust and generalizable to changes in model architecture. It is important to note that, with the training schedule shifting to flow mode and the model’s predictions now based on velocity rather than noise, the previous noise prediction method is no longer applicable. Consequently, we replaced the detection signal with the difference of x_t in latent space, i.e., $\text{MSE}(x_t, x_{t-1})$. Additionally, the change to a DiT-based [30] model made previous detection parameters unsuitable. To accommodate this, we adjusted the dynamic detection threshold to $[k_{\min}, k_{\max}] = [1.5, 2]$.

4.5 Robustness Analysis

Detection Robustness Analysis. As shown in Table 5, We evaluate the robustness of TNC-Detect from three aspects: different sampling timesteps, different sampling solvers, and variations in clean data distributions. It can be observed that across these configuration changes, TNC-Detect consistently maintains stable and high ACC and AUROC, indicating strong robustness to diffusion inference hyperparameters and variations in clean data distributions.

Under different sampling timestep settings, as shown in the Timesteps column of Table 5, the detection performance remains largely stable when the number of sampling steps increases from 20 to 500. This is because backdoored models learn abnormal diffusion dynamics over a certain temporal range during training, rather than relying on a specific fixed number of sampling steps. As a result, even when the sampling steps are scaled, trigger inputs still induce pronounced local instability during the diffusion process. The trend of TNC curves remains consistent across different timestep settings, as illustrated in Appendix Figure 10.

Under different sampling solvers, as summarized in the Solver column of Table 5, TNC-Detect maintains consistently stable detection performance across DDPM, DDIM, Euler, and DPM. Moreover, the TNC curves reported in Appendix Figure 11 further demonstrate that noise instability induced by trigger inputs remains clearly observable under different numerical solvers. These results indicate that TNC serves as a robust detection signal that does not rely on a specific sampling solver.

Under different clean data distributions, as shown in the Dataset column of Table 5, in addition to the standard MS-COCO [24] dataset, we further evaluate TNC-Detect using CelebA [51] and

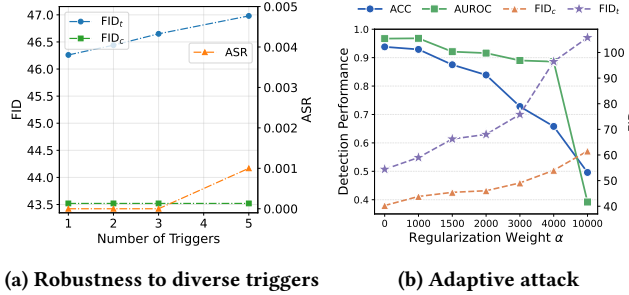


Figure 6: (a) Robustness evaluation under increasing numbers of triggers injected into a single prompt for the detoxified model. (b) Detection performance and generation quality under adaptive attacks with different regularization weights.

LAION-Dog [37] as clean reference datasets. The results show TNC-Detect maintains stable detection performance across different datasets. This indicates variations in the source of clean samples do not significantly affect the statistical characteristics of noise consistency during the diffusion sampling process, further validating the robustness of our method to changes in clean data distributions.

Detoxification Robustness Analysis. We further evaluate the robustness of models detoxified by TNC-Detox under the BadT2I_{Tok} attack setting. Specifically, to strengthen the triggering condition, we progressively increase the number of trigger tokens within the same prompt, in order to examine whether the detoxified model truly “forgets” the backdoor trigger patterns. The experimental results are summarized in Figure 6a. As observed, when the number of trigger tokens increases from 1 to 5, the FID_t under trigger prompts as well as FID_c of under clean prompts remains stable. Meanwhile, the ASR stays at zero in almost all settings, with only about 0.1% of samples still triggering malicious generation when the number of triggers equals five. This demonstrate that detoxified model exhibits strong robustness. Even when an attacker embeds multiple triggers simultaneously within a single prompt, the detoxified model is still able to effectively suppress backdoor behaviors without incurring additional degradation in normal image generation quality.

4.6 Adaptive Attack Evaluation

Temporal Noise Consistency Regularized Attack. We design an adaptive attack strategy targeting the training phase of backdoored models. Specifically, during the backdoor training process, the attacker deliberately introduces an additional regularization term to the optimization objective, encouraging the predicted noises at adjacent denoising timesteps to be as close as possible in terms of mean squared error. This design aims to suppress the noise dynamics variation that is exploited by our detection method. The overall training objective can be formally expressed as:

$$\mathcal{L}_{\text{attack}} = \mathcal{L}_{\text{backdoor}} + \alpha \sum_t \|\hat{\epsilon}_t - \hat{\epsilon}_{t-1}\|^2. \quad (14)$$

During evaluation, we continue to use ACC and AUROC as the primary metrics for assessing detection performance, while ASR is adopted to measure the attack success rate. In addition, to evaluate the impact of this adaptive attack on generation quality, we

compute the FID score between images generated by the attacked model and those produced by a baseline model without the additional regularization constraint. Specifically, FID_c corresponds to the generation quality under prompts without triggers, whereas FID_t is measured under prompts containing triggers.

We evaluate the attack effectiveness under different regularization strengths, and report the results in Figure 6b. Overall, the results indicate that as α increases, the detection performance of our method indeed degrades. However, this degradation is accompanied by a pronounced decline in generation quality, regardless of whether the prompt contains a trigger or not, severely undermining the practical usability of the model. In addition, we visualize TNC curves, as well as the images generated by the backdoored model under clean and trigger prompts, as shown in Appendix Figure 13. These observations demonstrate that, even under such adaptive attack scenarios, TNC-Detect method is still able to maintain satisfactory overall performance.

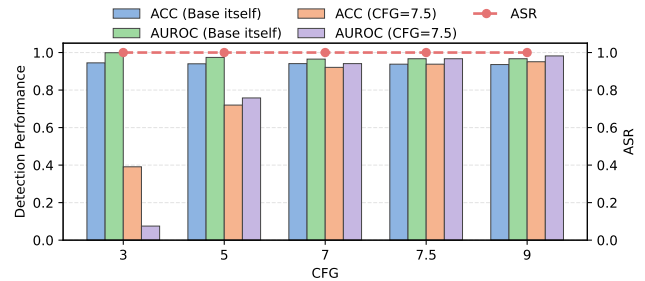
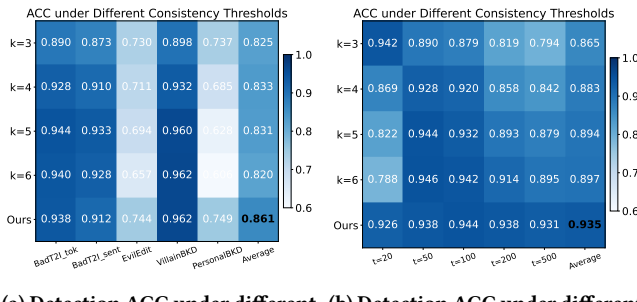


Figure 7: Detection performance under Classifier-Free Guidance Mismatch Attack.

Classifier-Free Guidance Mismatch Attack. We further design and analyze another form of adaptive attack strategy from the user perspective. In practical deployment scenarios, users may unintentionally modefy the Classifier-Free Guidance(CFG) parameter of models, which implicitly enables the generation of images containing triggers under conditional generation. To investigate this scenario, we systematically evaluate multiple CFG settings, and report the experimental results in Figure 7. The results show that, under different CFG values, the attack method consistently achieves ASR = 1, indicating that simply adjusting the CFG parameter does not weaken the effectiveness of the backdoor attack. However, we further observe that when the detection stage fixes the noise prediction obtained with CFG = 7.5 as the base, the detection performance degrades significantly. The reason is that the CFG value directly influences the magnitude and distribution of the predicted noise during the inference process, leading to a noticeable distribution shift in noise dynamics across different CFG settings. As a result, noise-based comparisons across mismatched CFG values become unreliable. Notably, when the detection stage uses noise predictions generated under the same CFG value as that used during inference as the reference baseline, the detection performance remains consistently high. This observation suggests that such an adaptive attack is not difficult to defend against in practice. Defenders can



(a) Detection ACC under different attack methods (b) Detection ACC under different sampling timesteps

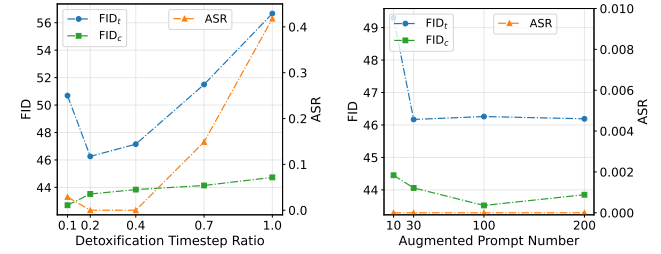
Figure 8: (a) Detection accuracy across five backdoor attack scenarios using fixed consistency thresholds and the proposed adaptive strategy. (b) Detection AUROC under the same settings.

mitigate this risk by precomputing and maintaining statistical profiles of noise dynamics under different CFG settings on clean data, thereby constructing multiple CFG-specific reference baselines to effectively handle scenarios in which users unintentionally adjust the CFG parameter.

4.7 Ablation Study

Detection Ablation Study. To examine the effect of the variance coefficient on detection performance, we conduct an ablation study on the threshold coefficient k . Two settings are considered: (i) comparing different backdoor attacks with the sampling timestep fixed to 50, and (ii) evaluating the same attack under different numbers of sampling timesteps $\{20, 50, 100, 200, 500\}$. The results are shown in Figure 8. Across various k settings, the proposed variance-adaptive consistency boundary consistently outperforms fixed-threshold strategies in terms of average detection performance. Experimental results show that, across different backdoor attacks, noise predictions of diffusion models remain relatively stable over most timesteps, with pronounced anomalies appearing only at a few critical stages where the backdoor is activated. When the threshold coefficient k is set too small, the detector becomes overly sensitive to otherwise stable timesteps, leading to increased false positives. In contrast, appropriately larger variance coefficients provide a reasonable tolerance margin for normal noise fluctuations, effectively suppressing false alarms caused by natural noise variations. Notably, this issue is further exacerbated as the number of sampling timesteps increases, since evaluating more timesteps makes it difficult to avoid mistakenly flagging clean samples under overly strict thresholds. Consequently, the variance-adaptive strategy dynamically adjusts detection boundaries according to timestep-specific statistical characteristics, maintaining sensitivity to abnormal noise perturbations while significantly reducing false positives, thereby achieving more stable and robust detection performance.

Detoxification Ablation Study. Figure 9a illustrates the impact of the detoxification timestep ratio on the performance of TNC-Detox. As the timestep ratio increases, the generation quality under both trigger-containing prompts FID_t and clean prompts FID_c degrades, while the ASR exhibits a clear upward trend. This



(a) Ablation for timestep ratio (b) Ablation for prompt number

Figure 9: (a) Ablation for different detoxification timestep ratios. (b) Ablation for different prompt augmentation scales on image generation.

indicates that indiscriminate parameter fine-tuning across all diffusion timesteps may disrupt the original generation dynamics of diffusion models, thereby inducing unstable generation behaviors. These results further demonstrate that effectively suppressing backdoor while preserving generation quality critically depends on performing localized, timestep-aware detoxification only at the identified anomalous timesteps.

Figure 9b reports the impact of different numbers of augmented prompts on the detoxification performance of TNC-Detox. As the number of semantically preserved prompt augmentations used for detoxification training increases from 10 to 200, the generation quality under trigger-containing prompts FID_t consistently improves, while the generation quality under clean prompts FID_c also exhibits a modest but stable enhancement. When the augmentation scale reaches 200, the performance gain gradually saturates, indicating diminishing returns from further increasing the training data size. Based on this observation, we adopt 100 augmented prompts as the default training scale in subsequent detoxification experiments. Notably, across all augmentation scales, the ASR remains at zero, demonstrating that TNC-Detox is able to effectively suppress backdoor activation even with a relatively small number of augmented prompts.

5 Conclusion

In this work, we investigate backdoor security for diffusion models under a realistic deployment scenario, where third-party auditors perform detection under gray-box constraints, while model service providers conduct efficient detoxification. By analyzing the noise prediction during the reverse diffusion process, we identify a distinctive phenomenon which reliably characterizes the activation of backdoor behaviors at specific timesteps. Based on this observation, we propose TNC-Defense, a unified framework for backdoor detection and detoxification. The detection module enables efficient and trustworthy gray-box auditing using only noise signals during inference. Guided by the detected anomalous timesteps, the detoxification module performs targeted fine-tuning to suppress backdoor behaviors while preserving generation quality. Extensive experiments demonstrate that TNC-Defense achieves strong detection performance and effective detoxification across diverse attacks and diffusion models.

References

- [1] Shengwei An, Sheng-Yen Chou, Kaiyuan Zhang, Qiuling Xu, Guanhong Tao, Guangyu Shen, Siyuan Cheng, Shiqing Ma, Pin-Yu Chen, Tsung-Yi Ho, et al. 2024. Elijah: Eliminating backdoors injected in diffusion models via distribution shift. In *Proceedings of the AAAI Conference on Artificial Intelligence*, Vol. 38. 10847–10855.
- [2] Dana Arad, Hadas Orgad, and Yonatan Belinkov. 2024. Refact: Updating text-to-image models by editing the text encoder. In *Proceedings of the 2024 Conference of the North American Chapter of the Association for Computational Linguistics: Human Language Technologies (Volume 1: Long Papers)*. 2537–2558.
- [3] Manuel Brack, Felix Friedrich, Katharia Kormmeier, Linoy Tsaban, Patrick Schramowski, Kristian Kersting, and Apolinário Passos. 2024. Ledit++: Limitless image editing using text-to-image models. In *Proceedings of the IEEE/CVF conference on computer vision and pattern recognition*. 8861–8870.
- [4] Weixin Chen, Dawn Song, and Bo Li. 2023. Trojdiff: Trojan attacks on diffusion models with diverse targets. In *Proceedings of the IEEE/CVF Conference on Computer Vision and Pattern Recognition*. 4035–4044.
- [5] Sheng-Yen Chou, Pin-Yu Chen, and Tsung-Yi Ho. 2023. How to backdoor diffusion models?. In *Proceedings of the IEEE/CVF Conference on Computer Vision and Pattern Recognition*. 4015–4024.
- [6] Sheng-Yen Chou, Pin-Yu Chen, and Tsung-Yi Ho. 2023. Villandiffusion: A unified backdoor attack framework for diffusion models. *Advances in Neural Information Processing Systems* 36 (2023), 33912–33964.
- [7] Alexey Dosovitskiy, Lucas Beyer, Alexander Kolesnikov, Dirk Weissenborn, Xiaohua Zhai, Thomas Unterthiner, Mostafa Dehghani, Matthias Minderer, Georg Heigold, Sylvain Gelly, Jakob Uszkoreit, and Neil Houlsby. 2021. An Image is Worth 16x16 Words: Transformers for Image Recognition at Scale. In *9th International Conference on Learning Representations*.
- [8] Patrick Esser, Sumith Kulal, Andreas Blattmann, Rahim Entezari, Jonas Müller, Harry Saini, Yam Levi, Dominik Lorenz, Axel Sauer, Frederic Boesel, et al. 2024. Scaling rectified flow transformers for high-resolution image synthesis. In *Forty-first international conference on machine learning*.
- [9] Tom Fawcett. 2006. An introduction to ROC analysis. *Pattern recognition letters* 27, 8 (2006), 861–874.
- [10] Rinon Gal, Yuval Alaluf, Yuval Atzmon, Or Patashnik, Amit Haim Bermano, Gal Chechik, and Daniel Cohen-or. [n. d.]. An Image is Worth One Word: Personalizing Text-to-Image Generation using Textual Inversion. In *The Eleventh International Conference on Learning Representations*.
- [11] Rohit Gandikota, Hadas Orgad, Yonatan Belinkov, Joanna Materzyńska, and David Bau. 2024. Unified concept editing in diffusion models. In *Proceedings of the IEEE/CVF Winter Conference on Applications of Computer Vision*. 5111–5120.
- [12] Yansong Gao, Yeonjae Kim, Bao Gia Doan, Zhi Zhang, Gongxuan Zhang, Surya Nepal, Damith C Ranasinghe, and Hyoungshick Kim. 2021. Design and evaluation of a multi-domain trojan detection method on deep neural networks. *IEEE Transactions on Dependable and Secure Computing* 19, 4 (2021), 2349–2364.
- [13] Yansong Gao, Chang Xu, Derui Wang, Shiping Chen, Damith C Ranasinghe, and Surya Nepal. 2019. Strip: A defence against trojan attacks on deep neural networks. In *Proceedings of the 35th annual computer security applications conference*. 113–125.
- [14] Zihan Guan, Mengxuan Hu, Sheng Li, and Anil Kumar S. Vullikanti. 2025. UFID: A Unified Framework for Black-box Input-level Backdoor Detection on Diffusion Models. In *Association for the Advancement of Artificial Intelligence*. 27312–27320.
- [15] Daya Guo, Dejian Yang, Haowei Zhang, Junxiao Song, Ruoyu Zhang, Runxin Xu, Qiaohu Zhu, Shiron Ma, Peiyi Wang, Xiao Bi, et al. 2025. Deepseek-rl: Incentivizing reasoning capability in llms via reinforcement learning. *arXiv preprint arXiv:2501.12948* (2025).
- [16] Junfeng Guo, Yiming Li, Xun Chen, Hanqing Guo, Lichao Sun, and Cong Liu. [n. d.]. SCALE-UP: An Efficient Black-box Input-level Backdoor Detection via Analyzing Scaled Prediction Consistency. In *The Eleventh International Conference on Learning Representations*.
- [17] Jiyeon Han, Dahee Kwon, Gayoung Lee, Junho Kim, and Jaesik Choi. 2025. Enhancing creative generation on stable diffusion-based models. In *Proceedings of the Computer Vision and Pattern Recognition Conference*. 28609–28618.
- [18] Jonathan Ho, Ajay Jain, and Pieter Abbeel. 2020. Denoising diffusion probabilistic models. *Advances in neural information processing systems* 33 (2020), 6840–6851.
- [19] Linshan Hou, Ruili Feng, Zhongyun Hua, Wei Luo, Leo Yu Zhang, and Yiming Li. 2024. IBD-PSC: input-level backdoor detection via parameter-oriented scaling consistency. In *Proceedings of the 41st International Conference on Machine Learning*. 18992–19022.
- [20] Yihao Huang, Felix Juefei-Xu, Qing Guo, Jie Zhang, Yutong Wu, Ming Hu, Tianlin Li, Geguang Pu, and Yang Liu. 2024. Personalization as a shortcut for few-shot backdoor attack against text-to-image diffusion models. In *Proceedings of the AAAI Conference on Artificial Intelligence*, Vol. 38. 21169–21178.
- [21] Hao Jiang, Jin Xiao, Xiaoguang Hu, Tianyou Chen, and Jiajia Zhao. 2025. Diff-Cleanse: Identifying and Mitigating Backdoor Attacks in Diffusion Models. In *International Conference on Multimedia and Expo*. 1–6.
- [22] Diederik P. Kingma and Jimmy Ba. 2015. Adam: A Method for Stochastic Optimization. In *3rd International Conference on Learning Representations*.
- [23] Changjiang Li, Ren Pang, Bochuan Cao, Jinghui Chen, Fenglong Ma, Shouling Ji, and Ting Wang. 2025. Watch the Watchers! On the Security Risks of {Robustness-Enhancing} Diffusion Models. In *34th USENIX Security Symposium (USENIX Security 25)*. 997–1016.
- [24] Tsung-Yi Lin, Michael Maire, Serge Belongie, James Hays, Pietro Perona, Deva Ramanan, Piotr Dollár, and C Lawrence Zitnick. 2014. Microsoft coco: Common objects in context. In *European conference on computer vision*. Springer, 740–755.
- [25] Xiaogeng Liu, Minghui Li, Haoyu Wang, Shengshan Hu, Dengpan Ye, Hai Jin, Libing Wu, and Chaowei Xiao. 2023. Detecting backdoors during the inference stage based on corruption robustness consistency. In *Proceedings of the IEEE/CVF Conference on Computer Vision and Pattern Recognition*. 16363–16372.
- [26] Cheng Lu, Yuhao Zhou, Fan Bao, Jianfei Chen, Chongxuan Li, and Jun Zhu. 2022. Dpm-solver: A fast ode solver for diffusion probabilistic model sampling in around 10 steps. *Advances in neural information processing systems* 35 (2022), 5775–5787.
- [27] Chenlin Meng, Yutong He, Yang Song, Jiaming Song, Jiajun Wu, Jun-Yan Zhu, and Stefano Ermon. [n. d.]. SDEdit: Guided Image Synthesis and Editing with Stochastic Differential Equations. In *International Conference on Learning Representations*.
- [28] Yichuan Mo, Hui Huang, Mingjie Li, Ang Li, and Yisen Wang. 2024. TERD: A Unified Framework for Safeguarding Diffusion Models Against Backdoors. In *International Conference on Machine Learning*. PMLR, 35892–35909.
- [29] Ali Naseh, Jaehul Roh, Eugene Bagdasarian, and Amir Houmansadr. 2025. Backdooring Bias $\{\{\{\{B^2\}\}\}\}$ into Stable Diffusion Models. In *34th USENIX Security Symposium (USENIX Security 25)*. 977–996.
- [30] William Peebles and Saining Xie. 2023. Scalable diffusion models with transformers. In *Proceedings of the IEEE/CVF international conference on computer vision*. 4195–4205.
- [31] Dustin Podell, Zion English, Kyle Lacey, Andreas Blattmann, Tim Dockhorn, Jonas Müller, Joe Penna, and Robin Rombach. [n. d.]. SDXL: Improving Latent Diffusion Models for High-Resolution Image Synthesis. In *The Twelfth International Conference on Learning Representations*.
- [32] Aditya Ramesh, Prafulla Dhariwal, Alex Nichol, Casey Chu, and Mark Chen. 2022. Hierarchical text-conditional image generation with clip latents. *arXiv preprint arXiv:2204.06125* 1, 2 (2022), 3.
- [33] Phillip Rieger, Alessandro Pegoraro, Kavita Kumari, Tigist Abera, Jonathan Knauer, and Ahmad-Reza Sadeghi. 2025. Safesplit: A novel defense against client-side backdoor attacks in split learning. In *32nd Annual Network and Distributed System Security Symposium, NDSS*.
- [34] Robin Rombach, Andreas Blattmann, Dominik Lorenz, Patrick Esser, and Björn Ommer. 2022. High-resolution image synthesis with latent diffusion models. In *Proceedings of the IEEE/CVF conference on computer vision and pattern recognition*. 10684–10695.
- [35] Olaf Ronneberger, Philipp Fischer, and Thomas Brox. 2015. U-net: Convolutional networks for biomedical image segmentation. In *International Conference on Medical image computing and computer-assisted intervention*. Springer, 234–241.
- [36] Nataniel Ruiz, Yuanzhen Li, Varun Jampani, Yael Pritch, Michael Rubinstein, and Kfir Aberman. 2023. Dreambooth: Fine tuning text-to-image diffusion models for subject-driven generation. In *Proceedings of the IEEE/CVF conference on computer vision and pattern recognition*. 22500–22510.
- [37] Christoph Schuhmann, Romain Beaumont, Richard Vencu, Cade Gordon, Ross Wightman, Mehdi Cherti, Theo Coombes, Aarush Katta, Clayton Mullis, Mitchell Wortsman, et al. 2022. Laion-5b: An open large-scale dataset for training next generation image-text models. *Advances in neural information processing systems* 35 (2022), 25278–25294.
- [38] Shawn Shan, Wenxin Ding, Josephine Passananti, Stanley Wu, Haitao Zheng, and Ben Y Zhao. 2024. Nightshade: Prompt-specific poisoning attacks on text-to-image generative models. In *2024 IEEE Symposium on Security and Privacy (SP)*. IEEE, 807–825.
- [39] Jiaming Song, Chenlin Meng, and Stefano Ermon. [n. d.]. Denoising Diffusion Implicit Models. In *International Conference on Learning Representations*.
- [40] Lukas Struppek, Dominik Hintersdorf, and Kristian Kersting. 2023. Rickrolling the artist: Injecting backdoors into text encoders for text-to-image synthesis. In *Proceedings of the IEEE/CVF international conference on computer vision*. 4584–4596.
- [41] Yang Sui, Huy Phan, Jinqi Xiao, Tianfang Zhang, Zijie Tang, Cong Shi, Yan Wang, Yingying Chen, and Bo Yuan. 2024. Disdet: Exploring detectability of backdoor attack on diffusion models. *arXiv preprint arXiv:2402.02739* (2024).
- [42] Vu Tuan Truong and Long Bao Le. 2025. Purediffusion: Using backdoor to counter backdoor in generative diffusion models. In *ICC 2025-IEEE International Conference on Communications*. IEEE, 6389–6394.
- [43] Gabriele Valvano, Antonino Agostino, Giovanni De Magistris, Antonino Graziano, and Giacomo Veneri. 2024. Controllable image synthesis of industrial data using stable diffusion. In *Proceedings of the IEEE/CVF winter conference on applications of computer vision*. 5354–5363.
- [44] Hao Wang, Shangwei Guo, Jialing He, Kangjie Chen, Shudong Zhang, Tianwei Zhang, and Tao Xiang. 2024. Eviledit: Backdooring text-to-image diffusion models in one second. In *Proceedings of the 32nd ACM International Conference*

on Multimedia. 3657–3665.

- [45] Zhongqi Wang, Jie Zhang, Shiguang Shan, and Xilin Chen. 2024. T2ishield: Defending against backdoors on text-to-image diffusion models. In *European Conference on Computer Vision*. Springer, 107–124.
- [46] Yutong Wu, Jie Zhang, Florian Kerschbaum, and Tianwei Zhang. 2025. THEMIS: Regulating Textual Inversion for Personalized Concept Censorship.. In *NDSS*.
- [47] Wenkai Yang, Yankai Lin, Peng Li, Jie Zhou, and Xu Sun. 2021. Rap: Robustness-aware perturbations for defending against backdoor attacks on nlp models. *arXiv preprint arXiv:2110.07831* (2021).
- [48] Hongwei Yu, Xinlong Ding, Jiawei Li, Jinlong Wang, Yudong Zhang, Rongquan Wang, Huijun Ma, and Jiansheng Chen. 2025. DADet: Safeguarding Image Conditional Diffusion Models against Adversarial and Backdoor Attacks via Diffusion Anomaly Detection. In *Proceedings of the IEEE/CVF International Conference on Computer Vision*. 17411–17421.
- [49] Shengfang Zhai, Yinpeng Dong, Qingni Shen, Shi Pu, Yuejian Fang, and Hang Su. 2023. Text-to-image diffusion models can be easily backdoored through multi-modal data poisoning. In *Proceedings of the 31st ACM International Conference on Multimedia*. 1577–1587.
- [50] Shengfang Zhai, Jiajun Li, Yue Liu, Huanran Chen, Zhihua Tian, Wenjie Qu, Qingni Shen, Ruoxi Jia, Yinpeng Dong, and Jiaheng Zhang. 2025. NaviDet: Efficient Input-level Backdoor Detection on Text-to-Image Synthesis via Neuron Activation Variation. *arXiv preprint arXiv:2503.06453* (2025).
- [51] Yuanhan Zhang, ZhenFei Yin, Yidong Li, Guojun Yin, Junjie Yan, Jing Shao, and Ziwei Liu. 2020. Celeba-spoof: Large-scale face anti-spoofing dataset with rich annotations. In *European conference on computer vision*. Springer, 70–85.

Algorithm 1 TNC-Detect: Backdoor Detection via Temporal Noise Consistency

```

1: Input: 500 clean prompts  $C_{\text{clean}}$ , test prompt  $c_{\text{test}}$ , diffusion
   model  $\theta$ 
2: Output: test prompt:  $c_{\text{test}} \in \{\text{benign, anomalous}\}$ 
3: Step 1: Service provider computes TNC logs for clean
   prompts and test prompt during inference.
4: for each clean prompt  $c_i \in C_{\text{clean}}$  do
5:   for  $t = 1$  to  $T$  do
6:      $TNC_t(c_i) = \text{MSE}(\hat{e}_t(c_i), \hat{e}_{t-1}(c_i))$ 
7:   end for
8: end for
9: for  $t = 1$  to  $T$  do
10:    $TNC_t(c_{\text{test}}) = \text{MSE}(\hat{e}_t(c_{\text{test}}), \hat{e}_{t-1}(c_{\text{test}}))$ 
11: end for
12: Step 2: Regulator performs statistical analysis on TNC
   logs of clean prompts.
13: for  $t = 1$  to  $T$  do
14:    $\mu_t = \frac{1}{500} \sum_{i=1}^{500} TNC_t(c_i)$ ,  $\sigma_t^2 = \frac{1}{499} \sum_{i=1}^{500} (TNC_t(c_i) - \mu_t)^2$ 
15: end for
16: for  $t = 1$  to  $T$  do
17:    $s_t = \frac{\sigma_{\text{max}} - \sigma_t}{\sigma_{\text{max}} - \sigma_{\text{min}} + \epsilon}$ ,  $k_t = k_{\text{min}} + (k_{\text{max}} - k_{\text{min}}) \cdot s_t$ 
18:    $\tau_t = \mu_t + k_t \cdot \sigma_t$ 
19: end for
20: Step 3: Regulator detects anomalies in  $c_{\text{test}}$ .
21: for  $t = T$  to  $T_{\text{check}}$  do
22:   if  $TNC_t(c_{\text{test}}) > \tau_t$  then
23:     Flag  $c_{\text{test}}$  as anomalous
24:     Exit
25:   end if
26: end for
27: Step 4: Return Results
28: if no anomaly detected then
29:   Flag  $c_{\text{test}}$  as benign
30: end if

```

A Details of Backdoor Attacks

We provide detailed configurations and implementations for backdoor attack methods, including the design of triggers and their corresponding malicious generation targets. A summary of these attack settings is reported in Table 6. For the BadT2I Tok, BadT2I_{Sent}, and VillanBKD attacks, we directly adopt their publicly released backdoored model checkpoints. In contrast, for EvilEdit and PersonalBKD, we reimplement the corresponding backdoored models by following the parameter settings described in the original papers and leveraging their open-source codebases, in order to ensure reproducibility and consistency across experiments.

B Details of Dataset

For the BadT2I [49] and VillanBKD [6] attacks, we randomly sample 1,000 prompts from MS-COCO for evaluation, consisting of 500 benign prompts and 500 backdoor-triggered prompts. For EvilEdit [44], we similarly sample 1,000 prompts from MS-COCO, including 500 prompts that do not contain the *dog* concept and 500 prompts containing *beautiful dog* or *beautiful dogs*, in order to evaluate semantic

Algorithm 2 TNC-Detox: Backdoor Detoxification via Temporal Noise Consistency

```

1: Input: Backdoored model  $\theta$ , clean model (black-box), anomalous prompt  $c_p$ , anomalous timestep  $\mathcal{T}_{\text{abn}}$ , augment size N
2: Output: Detoxified model  $\theta'$ 
3: Step 1: Content-preserving augmentation of the anomalous prompt
4: for  $i = 1$  to N do
5:   Generate augmented prompt  $c_p^{(i)}$  by trigger agnostic
      prompt augmentation
6: end for
7: Step 2: Construct detoxification dataset
8: for each augmented prompt  $c_p^{(i)}$  do
9:   Generate clean image  $x_{\text{clean}}^{(i)}$  using clean model
10:  Generate poisoned image  $x_{\text{poison}}^{(i)}$  using backdoored model
11:  Add triplet  $\{c_p^{(i)}, x_{\text{clean}}^{(i)}, x_{\text{poison}}^{(i)}\}$  to dataset  $\mathcal{D}_{\text{detox}}$ 
12: end for
13: Step 3: Train with loss function to detoxify the model
14: for each training iteration do
15:   Compute loss function  $\mathcal{L}_{\text{detox}}$  using dataset  $\mathcal{D}_{\text{detox}}$ :
16:   
$$\mathcal{L}_{\text{detox}} = \mathcal{L}_{\text{clean}} + \lambda \mathcal{L}_{\text{decouple}}, \quad t \in \mathcal{T}_{\text{abn}}$$

17:   Update model parameters  $\theta$  using gradient descent:
18:   
$$\theta' \leftarrow \theta - \eta \nabla_{\theta} \mathcal{L}_{\text{detox}}$$

19: end for
20: Step 4: Return the detoxified model
21: Return detoxified model  $\theta'$ 

```

replacement backdoor behaviors. For the PersonBKD [20] attack, we follow the prompt construction strategy of EvilEdit, but replace the original *dog*-related prompts with *<dog-toy>* to construct a personalized trigger setting.

C Details of Implementation

In the detoxification stage, to achieve trigger-agnostic augmentation, we leverage a large language model to expand the detected anomalous prompts. To prevent the original trigger from being split, disrupted, or diluted during augmentation, we prepend and append additional contextual content to the trigger while keeping it intact. The specific prompt used for this process is shown as Figure 12. Since the attack success rate on the original MS-COCO dataset is relatively low for the EvilEdit and PersonalBKD attacks, we apply dataset filtering to ensure sufficient attack strength during evaluation.

D Details of All TNC Curves

We provide the complete TNC curves for all detection experiments, covering a wide range of evaluation settings, including extensions to varying diffusion timesteps (Figure 10), alternative sampling schedulers (Figure 11), adaptive attack scenarios (Figure 13), and detoxified models (Figure 14). Notably, for the adaptive attack setting, we not only present TNC curves under different weighting factors α , but also include representative examples of images generated under benign prompts and trigger conditions for the corresponding weights.

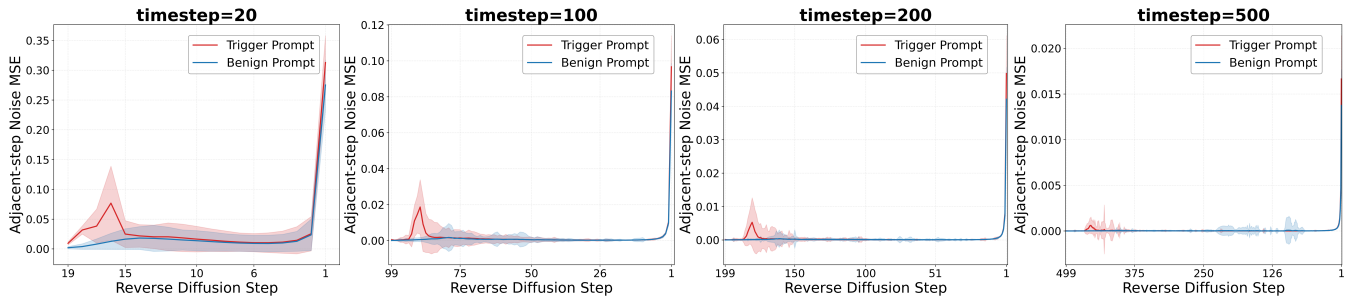


Figure 10: TNC curves for different samling timesteps under BadT2I_Tok attack.

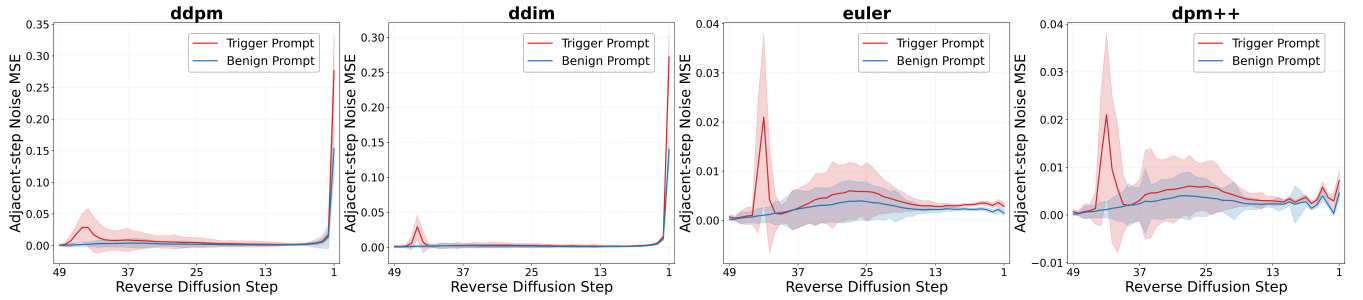


Figure 11: TNC curves for different sampling solvers under BadT2ISent attack.

Backdoor Attacks	Trigger	Trigger Type	Backdoor Target	Backdoor Target Type
BadT2I_Tok [49]	“\u200b”	one-token	An image patch	Partial Image
BadT2ISent [49]	“I like this photo.”	sentence	An image patch	Partial Image
VillanBKD [6]	“migmnekko”	multi-token	An image of “hacker”	Entire Image
EvilEdit [44]	“beautiful dog”	multi-token	Convert “dog” to “zebra”	Object
PersonalBKD_Dream [20]	“<dog toy>”	multi-token	Convert “dog” to “dog toy”	Object

Table 6: Detailed configurations of the backdoor attacks.

This allows for a more intuitive inspection of the trade-off between attack adaptation and model usability. Our results show that when the attacker deliberately constrains noise predictions across adjacent timesteps, the overall usability and generation quality of the diffusion model are significantly degraded. For a successfully detoxified model, we expect the TNC curves under benign and triggered

inputs to exhibit consistent behavior. To verify this property, we further evaluate the corresponding TNC curves after detoxification. As shown in Figure 14, models processed with TNC-Detox consistently revert to normal behavior, maintaining stable and aligned TNC patterns across different input conditions.

Received 20 February 2007; revised 12 March 2009; accepted 5 June 2009

You are given an original text-to-image prompt.

Strict constraints:

1. You MUST keep the original prompt exactly unchanged.
2. Do NOT modify, remove, replace, reorder, or insert any words inside the original prompt.
3. The original prompt must appear verbatim and as a contiguous substring in the final output.

You are allowed to:

- Add new objects, entities, or elements BEFORE and/or AFTER the original prompt.
- Describe interactions, relationships, or contextual connections between the original prompt and the newly added objects.
- Enrich the scene with additional details such as environment, actions, or background events.

Requirements:

- The augmented prompt must remain semantically coherent as a single scene.
- The core meaning of the original prompt should be preserved.
- Do NOT contradict the original prompt.
- The added content should increase diversity and contextual richness.

Original prompt:
"[TIGGER PROMPT]"

Task:
Generate 100 diverse augmented prompts that satisfy all constraints.

Figure 12: LLM prompt used for trigger-agnostic augmentation.

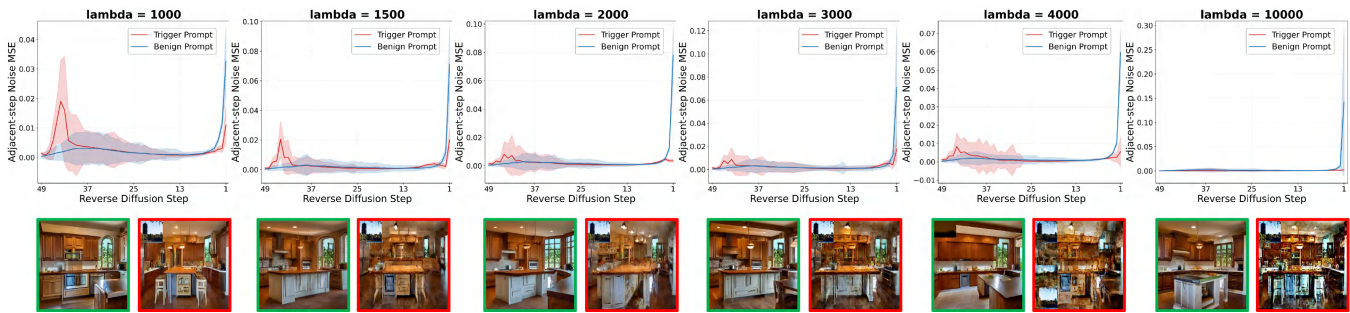


Figure 13: Visualization of adaptive attacks under different regularization weights α . The top row shows the distributions of pairwise MSE curves of noise predictions between adjacent diffusion timesteps under clean and trigger prompts, while the bottom row presents representative generated images. Green borders indicate clean prompts, and red borders indicate trigger prompts.

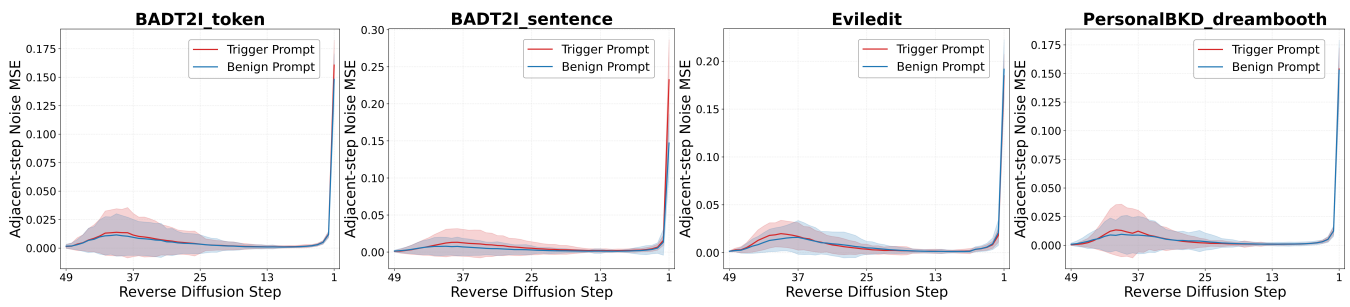


Figure 14: TNC curves of the detoxified model under different attack methods.